

# Fabrication of indium tin oxide bump/pit structures on GaN-based light emitting diodes

Zhe Liu, Yujin Wang, Haifang Yang,<sup>a)</sup> Hongxing Yin, Baogang Quan, Xiaoxiang Xia, Wuxia Li, and Changzhi Gu<sup>b)</sup>

*Beijing National Laboratory for Condensed Matter Physics, Institute of Physics, Chinese Academy of Sciences, P.O. Box 603, Beijing 100190, China*

(Received 29 June 2012; accepted 3 December 2012; published 19 December 2012)

In the past several decades, significant progress has been made to improve the performance of semiconducting light emitting diodes (LEDs), which has resulted in a wide number of applications for LEDs in the information and energy fields. However, light extraction efficiency is limited due to remarkable total internal reflection on the device's surface due to the large refractive index of GaN and indium tin oxides (ITO). In this work, ITO bump and pit patterns were fabricated on the LED surface using an ion beam etching method via metal or resist masks, respectively. By changing the incident angle of the ion beam and the material of the masks, the effects of faceting and redeposition can be properly controlled, resulting in well-controlled manipulation of the shape of the fabricated bump/pit structures. By altering the etching time, the over-etched structures have a much smoother surface compared with the under-etched/in-etched structures. These bump/pit structures could have potential applications in LED light emitting enhancement and optical devices. © 2013 American Vacuum Society. [<http://dx.doi.org/10.1116/1.4772462>]

## I. INTRODUCTION

GaN-based light emitting diodes (LEDs) are solid-state lighting devices which have excellent properties such as a long lifetime, low heat output, and low energy consumption.<sup>1</sup> They have attracted much attention in past decades and have been used in various applications such as mobile phones, monitors, and traffic lights. Although the internal quantum efficiency of GaN-based LEDs has reached over 70%,<sup>2</sup> the light extraction efficiency (LEE) is still very low due to total internal reflection in the air/dielectric interface. Generally, an indium tin oxide (ITO) top contact layer is deposited on the LED surface for current expansion because of the poor electrical conductivity of p-GaN, thus surface texturing and patterning of the ITO layer plays an important role in the value of the LEE. Various ordered and disordered ITO structures have been fabricated by wet chemical etching or inductively coupled plasma reactive ion etching (ICP-RIE) processes.<sup>3–8</sup> Wet etching has a good input–output ratio but lacks controllability in achieving designed structure profiles. The process of ICP-RIE is an effective method for ITO etching with a high etching rate and good selectivity; however, the incident direction of the reactive ions is always normal to the sample, which does not provide flexibility for controlling the geometry of ITO patterns.

Ion beam etching (IBE) is a method utilizing the interaction between incident ions and target materials and has been widely used to obtain textured surfaces.<sup>9–11</sup> One of the most suitable systems for IBE is based on the Kaufman type ion source.<sup>12</sup> In such a system, the ion flux and ion energy can be easily measured and controlled independently. What is more, the direction of ion bombardment with respect to the sample surface can be adjusted since the region around the

substrate is nearly free of electric field.<sup>13</sup> Through optimizing the faceting and redeposition effects during IBE, the profile of fabricated surface structures can be modified effectively.<sup>9</sup>

In this work, a technique to fabricate ITO bump/pit structures on LED surfaces based on an IBE system was developed. Metal and photoresist patterns were used as etching masks to produce bumps and pits, respectively. The faceting and redeposition effects were studied by changing the ion beam incident angle, the mask material and the thickness of the mask. Through optimizing the process, bump and pit structures with different cross-sectional profiles and pattern periods ranging from 350 to 750 nm were fabricated on the ITO layer of GaN-based LEDs.

## II. EXPERIMENT

The schematic diagram of the fabrication process is shown in Fig. 1. First, an ITO layer with a thickness of 460 nm was deposited on top of the p-GaN layer of a GaN-based LED, followed by spin-coating a 220-nm-thick layer of PMMA (polymethylmethacrylate) resist, then the sample was pre-baked on a hot-plate at 180 °C for 60 s [Fig. 1(a)]. Second, hole-arrays with periods ranging from 350 to 750 nm were formed on the PMMA layer [Fig. 1(b)] by a Raith 150 electron beam lithography (EBL) system. After exposure, the sample was developed in methyl isobutyl ketone:isopropyl alcohol (IPA) (1:3) for 40 s and IPA for 30 s, and then blown dry using pure nitrogen. Next, using electron beam evaporation [Fig. 1(c)] and a lift-off process, masks of metal plates were formed on the ITO layer [Fig. 1(d)]. Both the metal plates and PMMA holes were used as etching masks for the ion beam etching process (IBE system, LKJ-3D-150, ADVANCED) to get bump and pit structures, as shown in Figs. 1(e) and 1(f), respectively. The IBE system used in this work has a 4 in. Kaufman ion source, using argon as the operating gas. In the etching process, the current density was kept at 0.5 mA/cm<sup>2</sup>, the ion energy was set at 300 eV, the

<sup>a)</sup>Electronic mail: hfyang@iphy.ac.cn

<sup>b)</sup>Electronic mail: czgu@iphy.ac.cn

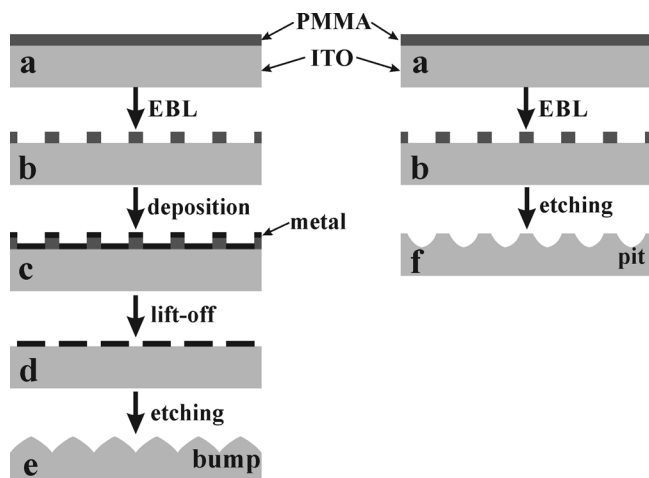


Fig. 1. Schematic diagram of the fabrication process.

working pressure was kept at 0.02 Pa, the sample holder was inclined from  $0^\circ$  to  $80^\circ$  with respect to the incident ions and kept rotating, and the working temperature was sustained at  $5^\circ\text{C}$ .

### III. OPTIMIZATION AND RESULTS

In contrast to the chemical etching process in the ICP-RIE system, IBE technology mainly depends on the target material and the related bombardment-based ion-matter interaction. There are two effects in the IBE process, namely, the faceting effect and the redeposition effect. As for the influence of the faceting effect, the corners of the mask patterns are eroded laterally by ion bombardment which causes a rapid change of the pattern geometry, so conic or hemispheric shaped structures can be fabricated. For the redeposition effect, the sputtered material is redeposited on sidewalls of the mask patterns, resulting in “crowns” or “wings” along the edges of the mask patterns.<sup>9</sup> The faceting and redeposition effects are closely related to the ion incident angle, the material type, and the thickness of the mask; thus, by optimizing these parameters, ITO bump/pit structures with different profiles can be obtained.

#### A. Tilt angle optimization

To examine the influence of the tilt angle on the etching rate and profile of the fabricated structures, IBE was performed on samples at tilt angles of  $0^\circ$ ,  $20^\circ$ ,  $40^\circ$ ,  $60^\circ$ , and  $80^\circ$ . It was found that the ion beam etching rate is highly related to the ion incident angle, as shown in Fig. 2. The inset in Fig. 2 shows the definition of the ion incident angle,  $\theta$ , which is equal to the tilt angle of the sample holder. The data demonstrate that the etching rate of ITO decreases with increasing tilt angle. This is because the effective ion flux and the pure elastic reflection of the incoming ions are closely related to the ion beam incident angle, which play an important role in the ion induced-collision cascade during the etching process.<sup>14</sup> We would like to point out that the etching rate was extremely low when the beam was incident at an angle of  $80^\circ$ . To avoid the instability of the ion source for long-time etching,  $80^\circ$  tilt angles were not used thereafter.

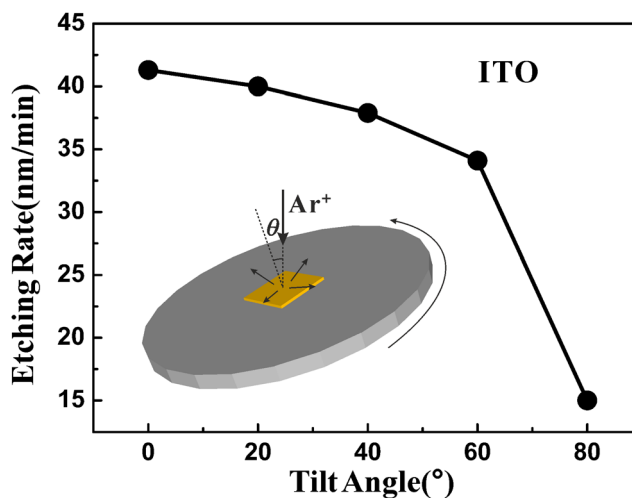


Fig. 2. (Color online) Etching rate of ITO as a function of the tilt angle. The definition of the tilt angle is shown in the inset.

In order to obtain sphere-like bump/pit profiles, etching times of 4, 3.5, 3, and 5 min were used for tilt angles which ranged from  $0^\circ$  to  $60^\circ$ . These etching time values were chosen so that the masks were scarcely etched over. The scanning electron microscope (SEM) images of textured ITO patterns are shown in Fig. 3, which were acquired at a viewing angle of  $52^\circ$ . The ITO bumps and pits have very sharp tips or bottoms when using a tilt angle of  $0^\circ$ . With increasing tilt angle, arc-shaped bumps and pits can be achieved. In fact, both the top and bottom parts of the structures show a faceting effect.<sup>15</sup> By changing the tilt angle, faceting and redeposition effects can be tuned, which can lead to the formation of structures with various controllable profiles. At a

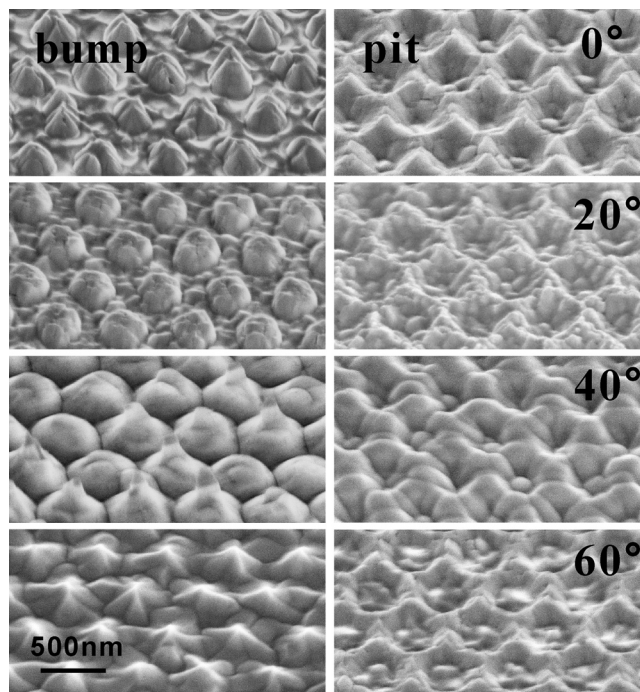


Fig. 3. SEM images of the bump and pit structures with a period of 750 nm. These were etched at different tilt angles using Cr and PMMA masks, respectively.

tilt angle of  $0^\circ$ , since the ions strike the sidewalls at a glancing angle with a low etching rate, the projectiles of the target atoms are confined and the recapture of sputtered atoms is predominant, resulting in an inclined sidewall. After the top of the masks is laterally eroded, cone-shaped bumps and pits are formed. By further increasing the tilt angle, the situations for bumps and pits are different. For bump structures at a large tilt angle, the etching of the sidewall is enhanced leading to a new balance between sputtering and redeposition on the pattern sidewalls, and thus, the profile of the structures change accordingly. When the tilt angle is increased up to  $60^\circ$  the etching rate on the flat surface decreases but lateral etching is still remarkable, reducing the height of the formed bumps. Therefore, small tilt angles are used to obtain conic profiles, while large tilt angles achieve spherical profiles. However, further increasing the tilt angle would finally ruin the shape of the etched structures.

Other than bumps, the pit structures have some differences. The PMMA mask for pits was much thicker (220 nm) than the Cr mask (70 nm) used for bumps. For hole arrays with diameters of only several hundred nanometers, at large incident angles the incident ion beam is mainly blocked by the sidewall of the mask pattern and cannot reach the bottom of the ITO layer, so it is hard to get well-profiled pit structures using a tilt angle of  $40^\circ$ . However, nice pit structures can be achieved at a tilt angle of  $0^\circ$ , as shown in Fig. 3. Therefore, in order to achieve the desired structural profile, the thickness of the mask should be carefully considered.

## B. Materials of masks

To take advantage of the effects of faceting and redeposition in structure fabrication, it is also important to choose suitable mask materials. A mask with a high etching selectivity to the target material can reduce faceting effects, while those with small thicknesses can reduce the redeposition effect.<sup>9</sup> For most materials, the etching rate first increases, then reaches a maximum, and finally decreases as the ion beam incident angle is increased.<sup>14</sup> Figure 4 shows the etching rate of Ti, Cr, and Au as a function of tilt angle, which were obtained with an ion beam energy of 300 eV and an ion current of  $0.5 \text{ mA/cm}^2$ . It can be seen that Ti has the smallest etching rate and Au has the largest one.

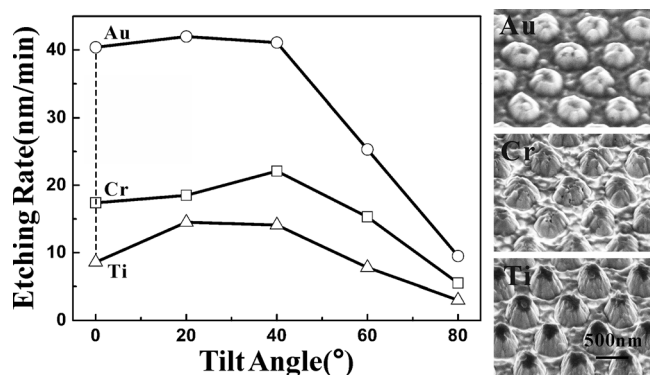


FIG. 4. Etching rate of different materials as a function of tilt angle. Structures shown in the SEM images were etched at a tilt angle of  $0^\circ$  with a period of 550 nm.

In order to investigate the effect of the mask material, Ti (50 nm), Cr (70 nm), and Au (150 nm) metal patterns were used, and the thickness of each material was chosen so that all of them required the same etching time of 4 min to be scarcely etched over. Figure 4 shows the SEM images of bump structures with different etching mask materials at a tilt angle of  $0^\circ$ . It shows that the bumps fabricated by the Ti mask have the steepest sidewalls, but those formed with the Au masks are semi-spherical. Such phenomena can be explained by the dynamic interrelation of the faceting and redeposition effects. Since the selectivity of Ti to the substrate material is much higher than that of Au, the faceting effect is much less obvious. As for the Cr mask, the edge was eroded faster than that of the Ti mask so the bumps became semisphere-like. In addition, Au (with smallest selectivity) has the largest thickness and thus, the ejected material tends to redeposit on the sidewalls and edges of the mask. The redeposited material was difficult to sputter away again due to the blocking of the incident beam by the mask sidewall, so the profile of the target structure became rounded.

## C. Fabrication results

It has been demonstrated above that ITO structures with different profiles can be obtained using optimized etching conditions with proper mask materials and pattern structures. Figures 5(a) and 5(b) show the bump and pit structures with different periods which were etched at a tilt angle of  $20^\circ$  using Cr (thickness of 70 nm) and PMMA (thickness of

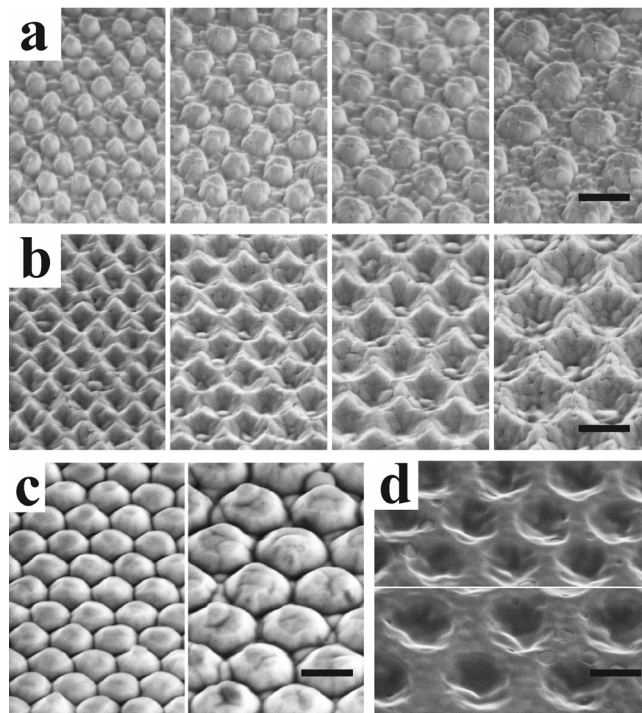


FIG. 5. (a) SEM images of ITO bumps with periods of 350, 450, 550, and 750 nm, etched at a tilt angle of  $20^\circ$ , using a Cr mask. (b) SEM images of ITO pits with periods of 350, 450, 550, and 750 nm, etched at a tilt angle of  $20^\circ$ , using a PMMA mask. (c) SEM images of bumps over-etched at a tilt angle of  $40^\circ$  for 10 min. (d) SEM images of pits over-etched at a tilt angle of  $40^\circ$  for 14 min. The scale bar is 500 nm.

220 nm) pattern as masks, respectively. Meanwhile, it was found that by performing a sufficiently long etching time (over etching) at larger tilt angles, structures with much smoother surfaces can be obtained. Figure 5(c) shows the bumps that were etched at a tilt angle of 40° for 10 min using Cr (thickness of 70 nm) masks, and in Fig. 5(d), the pits were etched at a tilt angle of 40° for 14 min using 220 nm thick PMMA masks. These both show smoother surfaces compared with those under-etched/in-etched structures, which is due to the polishing effect of IBE.<sup>16</sup> These results suggest that IBE can fabricate multifarious textured ITO for light-emitting enhancement of LEDs or for use as microlens for optical devices.

#### IV. CONCLUSIONS

We have demonstrated the feasibility of fabricating ITO bump/pit structures on GaN-based LEDs by IBE. The ion beam incident angle, mask material, geometry of the mask patterns, and etching time were optimized to achieve desired ITO structures. It was found that using a small ion beam incident angle for etching could result in cone-like structures, while a large tilt angle is favorable to obtain structures with hemisphere-like shapes. Meanwhile, thick masks in conjunction with a large etching rate could enhance the redeposition effect and can be used to obtain bumps with round tops. In addition, over-etched structures were found to have a much smoother surface. These results indicate that an optimized fabrication process can be used to fabricate textured surfaces on LEDs for enhanced light emitting.

#### ACKNOWLEDGMENTS

This work was supported by the National Basic Research Program of China (Grant No. 2009CB930502) and National Natural Science Foundation of China (Grants Nos. 50825206, 1083401, 91023041, 61001045, and 11174362) and the Knowledge Innovation Project of CAS (Grant No. KJCX2-EW-W02).

- <sup>1</sup>S. Nakamura, *MRS Bull.* **34**, 101 (2009).
- <sup>2</sup>D. Fuhrmann, C. Netzel, U. Rossow, A. Hangleiter, G. Ade, and P. Hinze, *Appl. Phys. Lett.* **88**, 071105 (2006).
- <sup>3</sup>T. S. Kim, S. M. Kim, Y. H. Jang, and G. Y. Jung, *Appl. Phys. Lett.* **91**, 171114 (2007).
- <sup>4</sup>D. S. Leem, T. Lee, and T. Y. Seong, *Solid-State Electron.* **51**, 793 (2007).
- <sup>5</sup>K. J. Byeon, E. J. Hong, H. Park, K. Y. Yang, J. H. Baek, J. Jhin, C. H. Hong, H. G. Kim, and H. Lee, *Semicond. Sci. Technol.* **24**, 105004 (2009).
- <sup>6</sup>T. K. Kim *et al.*, *Appl. Phys. Lett.* **94**, 161107 (2009).
- <sup>7</sup>J. H. Kang, J. H. Ryu, H. K. Kim, H. Y. Kim, N. Han, Y. J. Park, P. Uthirakumar, and C. H. Houg, *Opt. Express* **19**, 3637 (2011).
- <sup>8</sup>K. H. Li and H. W. Choi, *J. Appl. Phys.* **110**, 053104 (2011).
- <sup>9</sup>M. E. Walsh, Y. Hao, C. A. Ross, and H. I. Smith, *J. Vac. Sci. Technol. B* **18**, 3539 (2000).
- <sup>10</sup>F. Stade, A. Heeren, M. Fleischer, and D. P. Kern, *Microelectron. Eng.* **84**, 1589 (2007).
- <sup>11</sup>Z. Liu, X. Xia, Y. Sun, H. Yang, R. Chen, B. Liu, B. Quan, J. Li, and C. Gu, *Nanotechnology* **23**, 275503 (2012).
- <sup>12</sup>H. R. Kaufman, J. M. E. Harper, and J. J. Cuomo, *J. Vac. Sci. Technol.* **16**, 179 (1979).
- <sup>13</sup>J. M. E. Harper, J. J. Cuomo, and H. R. Haufman, *Annu. Rev. Mater. Sci.* **13**, 413 (1983).
- <sup>14</sup>O. Auciello, *J. Vac. Sci. Technol.* **19**, 841 (1981).
- <sup>15</sup>A. R. Neureuther, C. Y. Liu, and C. H. Ting, *J. Vac. Sci. Technol.* **16**, 1767 (1979).
- <sup>16</sup>A. I. Stognij, N. N. Novitskii, and O. M. Stukalov, *Tech. Phys. Lett.* **28**, 17 (2002).